Fringe ATSR Workshop 2005

Opening Session

Official ESA Welcome *Stephen Briggs*

Workshop Objectives and Organization
Workshop presentation
Yves-Louis Desnos (ESA)

Opening Session: Presentations by ESA *Chair: Y.-L. Desnos/M. Engdahl*

ERS and Envisat missions status
Workshop presentation
Wolfgang Lengert (ERS Mission Manager)

ERS and Envisat missions: data and services
Workshop presentation
Henri Laur (Envisat Mission Manager)

ERS SAR - ENVISAT ASAR: Performance, Processing, Products for Interferometry
Workshop presentation
Betlem Rosich Tell (ESA)

INSAR services for GMES : utilisation of ERS and ENVISAT for pan-European subsidence monitoring
Workshop presentation
Philippe Bally (ESA)

Thematic Mapping and DEMs *Chair: J. Hoffmann/F.M. Seifert, sec. T. Pearson*

Analysis of InSAR phase coherence and correlation of image intensity in urban environment: effects of baseline and urban texture
Nazzareno Pierdicca (Univ. La Sapienza of Rome)

Damage Mapping Using Interferometric Coherence
Jörn Hoffmann (German Aerospace Center)

ERS-ENVISAT Cross-interferometry for Coastal DEM Construction
Workshop presentation
Sang-Hoon Hong (Yonsei University)

Urban DEM
Workshop presentation
Daniele Perissin (Politecnico di Milano)

On the generation of a forest biomass map for Northeast China: SAR interferometric processing and development of classification algorithm
Workshop presentation
Maurizio Santoro (Friedrich-Schiller University)

A DEM-Free Approach to Persistent Point Scatterer Interferometry
Mark Warren (University of Nottingham)

Implication of Secondary Geodynamic Phenomena on Co-seismic Interferometric Coherence
Issaak Parcharidis (Harokopio University of Athens)

The November 22, 1995, Mw = 7.2 Gulf of Elat (Aqaba) earthquake cycle revisited
Workshop poster
Gidon Baer (Geological Survey of Israel)

Measurement of a Small-scale Subsidence in a Reclaimed Land using RADARSAT-1 SAR
Chang-Wook Lee (Yonsei University)

Results of landslide detection based on SAR Interferometry processing
Workshop poster
Bjoern Riedel (TU Braunschweig)

Relationship between piezometric level and ground deformations measured by means of DInSAR in the Vega Media of the Segura River (Spain)
Roberto Tomás (Universidad de Alicante)

Atmospheric Effects on 35-Day Repeat Cycle ERS Interferograms of London
Jon Leighton (University of Nottingham)

Detection of subsidences and landslides in the North-Bohemian coal basin by the InSAR method
Workshop poster
Ivana Capkova (Faculty of Civil Engineering, Czech Tech. Univ.)

Application of SAR interferometry for studies of Caspian coast covers
Alexander Zakharov (IRE RAS)

Monitoring of gas pipelines state in Western Siberia using spaceborne SAR interferometry
Alexander Zakharov (IRE RAS)

Space-Adaptive coherence estimation
Andrea Monti Guarnieri (Politecnico di Milano)

Temporal Variability of Ice Flow on Hofsjökull, Iceland, observed by ERS SAR Interferometry
Florian Mueller (University of Innsbruck)

Kinematics, asperities and seismic potential of the Hayward fault, California from ERS and RADARSAT PS-InSAR
Gareth Funning (University of California)

Enhanced quick and dirty estimate for SAR coherence
Andrea Monti Guarnieri (Politecnico di Milano)

Coherence-based Methodology for Interferometric Dem Integration
Pablo Euillades (Instituto CEDIAC - Universidad Nacional de Cuyo)

Designing and Testing a Network of Omnidirectional Permanent Scatterers
Chuck Wicks (USGS)

Antarctic SAR and INSAR calibration experiment during the International Polar Year
Benoit Legresy (CNRS/Legos)

Application of ASAR-ENVISAT Data for Monitoring Andean Volcanic Activity : Results from Lastarria-Azufre Volcanic Complex (Chile-Argentina)
Jean-Luc Froger (IRD LMV UR163 / UMR6524)

The Preliminary Result on Persistent Scatters and Corner Reflectors Differential Interferometry in Three Gorges Area
Qiming Zeng (Peking University)

Urban Change Detection Using Coherence and Intensity Characteristics of Multi-temporal ERS-1/2 Imagery
Mingsheng Liao (Wuhan University)

Land subsidence monitoring in the Lucca plain (central Italy) with ERS and Envisat
Leonardo Disperati (Università di Siena - Centro di GeoTecnologie)

The Performance of ERS-1/2 Tandem SAR Coherence Image to Estimate Forest Volume Density in the Northeast of China
Yong Pang (Chinese Academy of Forestry)

Utilizing the CR-network in Iceland for an automated interferometric processing chain - Test case with ERS-Tandem data
Karlheinz Gutjahr (Joanneum Research)

Landslides

Chair: H. Rott/U. Wegmuller, sec. F. Palazzo

Long term DInSAR analysis of a deep seated gravitative motion in the Alpine region of Val Di Susa, Italy
Workshop presentation
Simone Atzori (INGV)

SAR Interferometric Point Target Analysis of Slope Instabilities in the Community of Biasca, Switzerland
Workshop presentation
Tazio Strozzi (Gamma Remote Sensing)

On the application of PSI technique to landslide monitoring in the Daunia mountains, Italy
Workshop presentation
Fabio Bovenga (Dip. Interateneo di Fisica - Bari)

Landslide hazard mapping at a basin scale using remote-sensing data and artificial neural networks
Workshop presentation
Sandro Moretti (Università di Firenze)

Future missions

Chair: G. Levrini sec. F. Sarti

TanDEM-X: A Satellite Formation for High Resolution SAR Interferometry
Workshop presentation
Gerhard Krieger (DLR)

Interferometric capabilities of ALOS PALSAR and its utilization
Workshop presentation
Ryoichi Furuta (JAXA)

RADARSAT-2: Mission Overview and Applications
Bernhard Rabus (MDA)

SAR Interferometry Capabilities of Canada's planned SAR Satellite Constellation
Workshop presentation
Dirk Geudtner (Canadian Space Agency)

Mission and System Characteristics of the European Radar Observatory (Sentinel-1)
Workshop presentation
Evert Attema (ESA)

Summary session

Session Summaries

Session Recommendations

LAND SUBSIDENCE MONITORING IN THE LUCCA PLAIN (CENTRAL ITALY) WITH ERS 1/2

Leonardo Disperati (*), Salvatore Virdis (*), Kurt L. Feigl (**) & Andrea Rindinella (*)

(*) Università di Siena, Centro di Geotecnologie, via Vetri Vecchi, 34 52027 San Giovanni Valdarno (Ar), Italia
disperati@unisi.it , www.geotecnologie.unisi.it
(**) CNRS UMR 5562, 14 ave E. Belin - 31400 Toulouse, France
feigl@dtp.obs-mip.fr

AIM

We present preliminary results of a project supported by ESA (Category 1 n. 3063) and Italian Ministry of Education, University and Research (COFIN 2003) in the Lucca plain, central Italy (Figure 1), to study land subsidence by integrating satellite radar interferometry with ground-truth leveling surveys.
The subsidence appears to be related to the withdrawal of groundwater over the last two decades, which caused drop of water table (Figure 2) and in turn led to elasto-plastic compaction of fine-grained sediments.

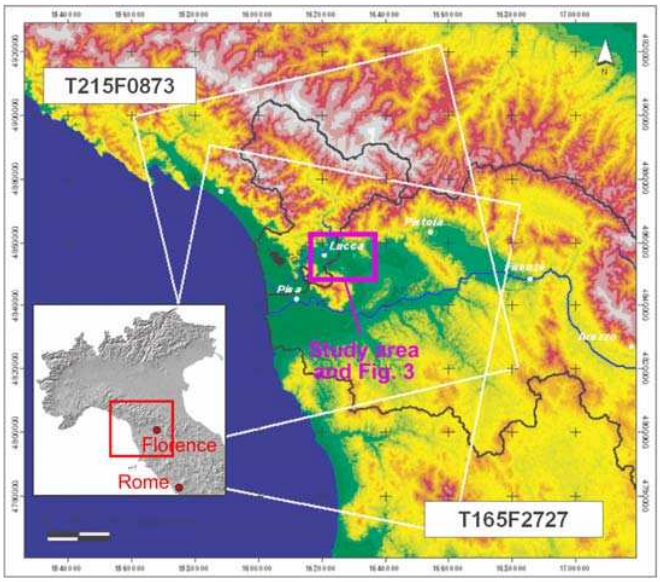

Figure 1. Study area and track & frame of the ascending and descending paths. Coordinate system: GAUSS-BOAGA projection, zone W).

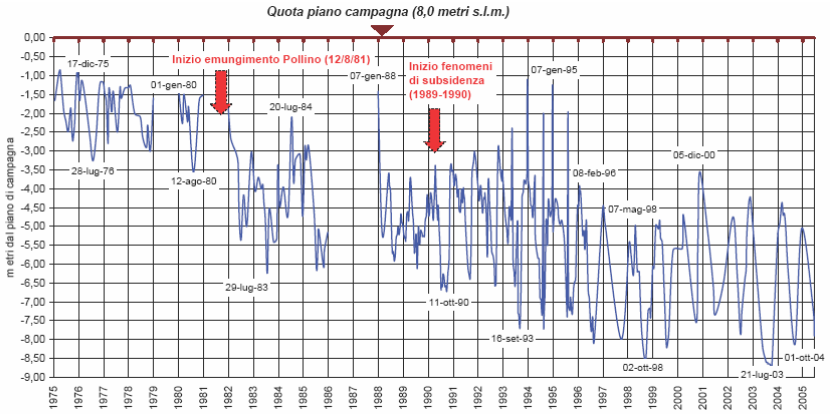

Figure 2. Water table changes in the "Pollino" well field, within the study area, monitored from 1975 to 2005 (from AdB Serchio River Authority).

GEOLOGY OF THE STUDY AREA

The Lucca plain is located within one of the extensional tectonic basins which dissect the inner part of the Northern Apennines. Recent continental deposits of the plain are made up of thick sandy gravel cropping out in the northern

sector of the plain overlain by a clayey silt horizon thickening toward the South. These deposits rest unconformably over units related to the Triassic Verrucano, the Triassic-Oligocene Tuscan Nappe, the Ligurides units (Cretaceous-Oligocene) and the "Villafranchian" sediments (Late Pliocene-Early Pleistocene) (Figure 3).
Normal faults located to the S and to the N of the area controlled the development of the plain until recent times. Hence regional vertical motions can be combined with subsidence caused by anthropogenic actions.

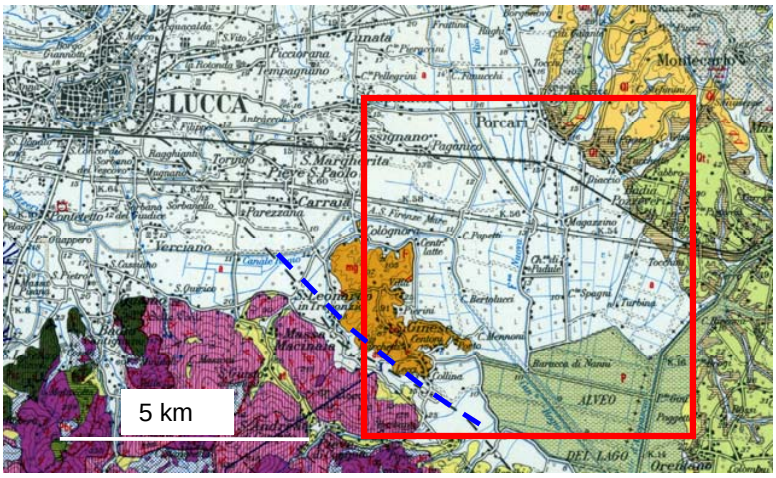

Figure 3. Geological map of the study area (*Carta Geologica d'Italia*, sheet 105). Legend of formations: Pf: phyllites and quartzites ("Filladi e quarziti di Buti", ? Carboniferous); Psc: continental conglomerates, phyllites ("Scisti di S. Lorenzo", l. Carboniferous - e Permian; Pbr: phyllites, breccias, conglomerates ("Brecce di Asciano", ? Permian); Tcg: quartz conglomerates and phyllites ("Formazione della Verruca, m. Trias); Tqz: clorite-sericite phyllites with quartzites ("Quarziti di M: Serra", Carnian); gr: dolostones and dolomitic limestones ("Grezzoni", l. Triassic); mg: sandstones and argillites ("Macigno", L. Oligocene-E. Miocene); alb + al: clays and marls with limestones, marly limestones, limestones ("Alberese", l. Cretaceous - Paleocene); Cmc: marly limestones and sandstones (l. Cretaceous); ar: sandstones with marls (? Cretaceous); Ql + Qfl1: gray clays, sandy clays and lacustrine sands with conglomerates; conglomerates, lacustrine clays ("Villafranchian"); Qt + Qt1: reddish sands, conglomerates and gravels (Pleistocene); Qfl2: fluvial-lacustrine gravelly, sandy and clayey deposits (Pleistocene); at: terraced deposits (Pleistocene); p + t: peat and marsh deposits (Olocene); a: recent continental deposits (Olocene). Blue dashed line: inferred normal fault. Red box: extent of the orthophoto in Figure 5.

DATA

In order to fulfil the objectives of the work we used the following data:

- Digital Elevation Model, cell size: 40 m.
- ERS 1/2 images:
  - ascending track 873, frame 215 (Figure 1);
  - descending track 165, frame 2727;

  pairs used in this work are listed in Figure 4.
- Aerial photographs and orthophotos from I.G.M.I. (*Istituto Geografico Militare Italiano*) and Regione Toscana.
- Ancillary data from technical reports of local municipalities, Arno and Serchio river basins authorities (leveling, soil mechanics, stratigraphic, hydrogeological and geophysical data).

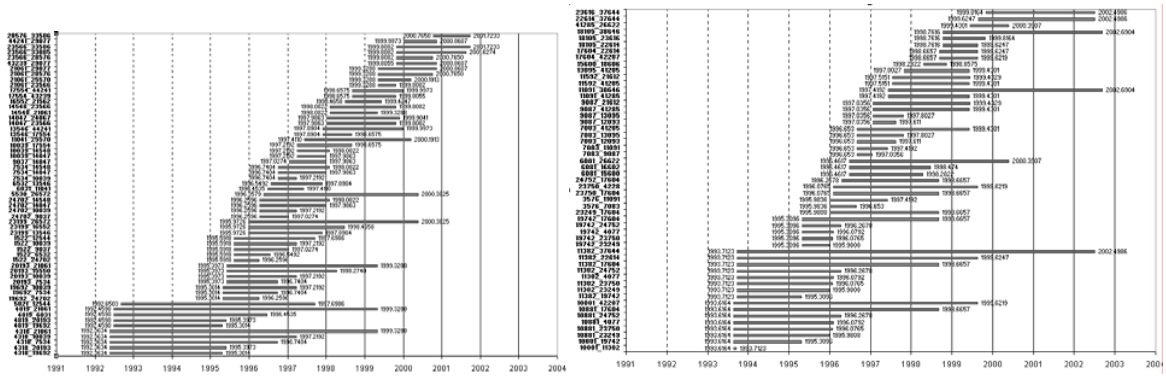

Figure 4. The interferometric dataset for the descending and ascending tracks.

LEVELING SURVEY

Between September-December 2004, we monumented a leveling network of 22 new benchmarks (indicated as **cs** in Figure 5). In order to allow us to monitor any vertical ground movements (regional geologic or anthropogenic) within the plain, the network connects Verrucano and Villafranchian outcrops located out of the south-western and nothern borders of the study area. The network integrates an existing network monitored between 1995 and 1996 (indicated as **csv** in Figure 5). Both the old and new networks were measured at the beginning of 2005. As ground truth we also took into account data from a leveling network located in the north-eastern part of the study area (Figure 5).

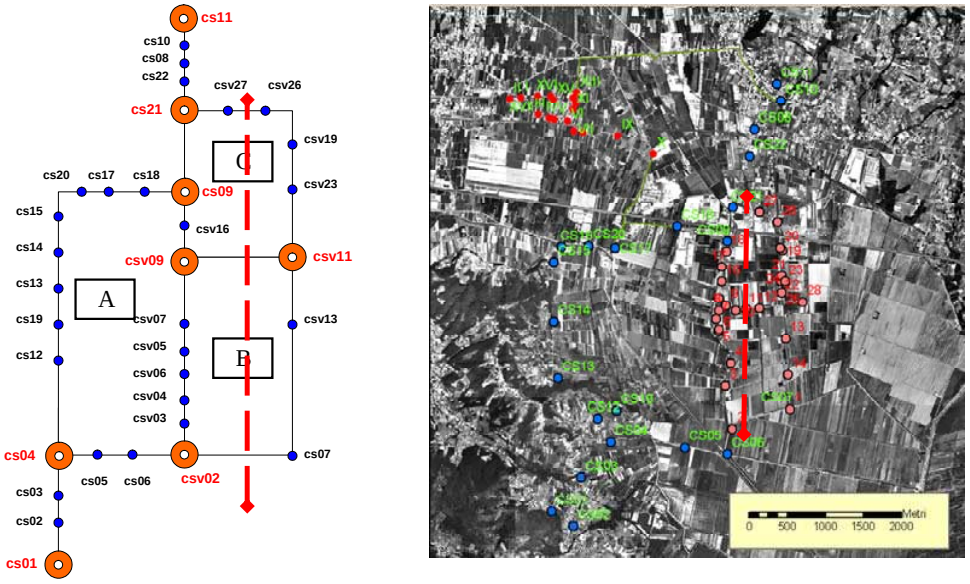

Figure 5: On the left the logical scheme of the network. On the right the leveling networks used in this works superimposed to the orthophotos. Red line: profile of Figure 6.

We followed the procedures suggested by the I.G.M.I. for high precision leveling survey (*Muller*, 1986):

a. leveling methodology is backward-forward.

b. misclosure error between forward and backward surveying should be less than $2.5\sqrt{L}$ mm (where L is distance expressed in Km);

c. all the benchmarks are closer than 1 Km;

In Figure 6 the results of leveling are reported:

- vertical benchmark displacement rates decrease with time (non-linear subsidence process);
- quite high spatial variability of subsidence;
- mean velocities measured: ca. 2-6 mm/year (higher rates close to the water pumping station of the so called “Pollino” wells field (Figure 2 and **csv**13 in Figure 5).

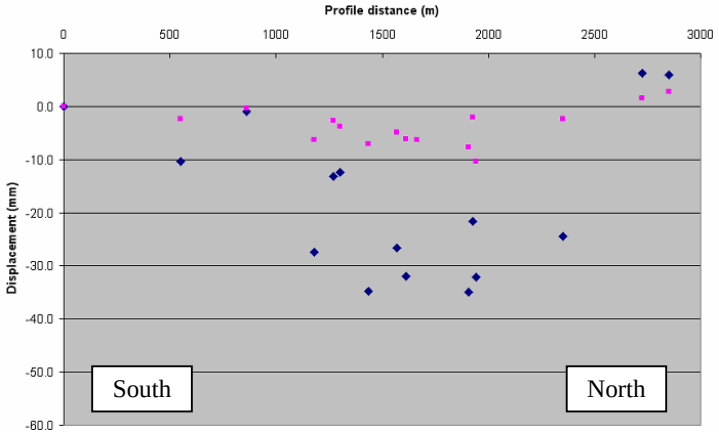

Figure 6. Vertical benchmarks displacement measured through leveling. Purple dots: benchmarks measured between 95 and 96; blue dots: benchmarks measured between 1995 and 2005

InSAR and TEMPORAL ADJUSTMENT

We calculated the interferograms (Figure 7) using the software DIAPASON developed by CNES, choosing the two-pass approach (*Massonnet e Feigl*, 1998). We used the following criteria for pair selection:

- abs(Ha) > 100 m
- abs(dDop) < 0.2 PRF
- Dtdays < 1000.

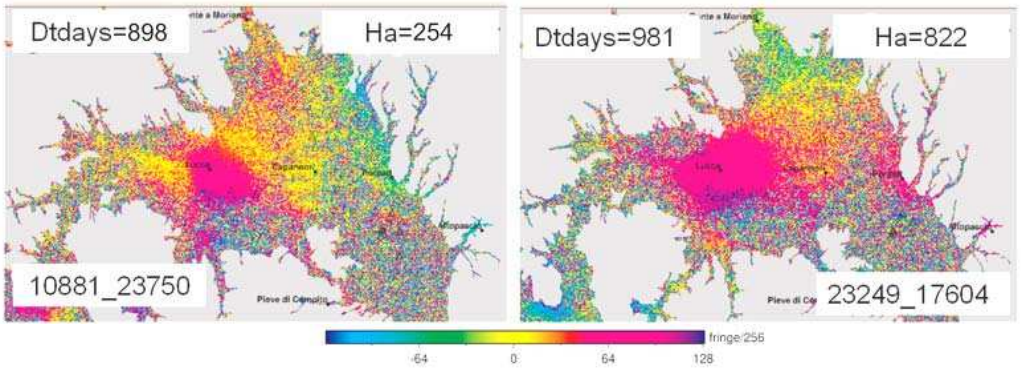

Figure 7. Examples of the interferograms calculated.

We unwrapped the phase values in a single spatial dimension (profile) using the Matlab routine unwrap. Accordingly, we converted the wrapped interferometric phase ϕ from the integer 8-bit value range [-128; +127] to an unwrapped range change $\Delta\rho$ in mm.

For the temporal approach, we analysed the difference in range change ($\Delta\rho$) between point K and point 1 of a profile denoted by $\Delta\Delta\rho_{ij} = [\Delta\rho_{ij}]_k - [\Delta\rho_{ij}]_1$ (*Feigl, et al.*, 2000) where *i* represents the index of the master epoch (t_i) and *j* the index of the slave epoch (t_j). The double delta denotes two differences, one in time (t_i - t_j) and one in space (point K - Point 1). We then performed a simple inversion of the linear model

$$\mathbf{Ax} = \Delta\Delta\rho_{ij}$$

where the parameters **x** pertain to epochs and the data $\Delta\Delta\rho_{ij}$ pertain to the time intervals spanned by the interferometric pairs. The design matrix **A** links the data and the parameters. For each row of **A**, the values are zero except for the columns corresponding to epochs *i* and *j* which are –1 and 1, respectively (*Usai*, 2003). For each pixel K, the problem is described by n parameters and m observations. The last line of **A** is filled by 1's to introduce a supplementary independent equation ($\Sigma\Delta\Delta\rho_{ij} = 0$) to regularize the solution.

1D phase unwrapping becomes unreliable or difficult to interpret in poorly correlated areas like the southern part of the Lucca plain. For this reason we selected Pseudo Invariant Features (PIF) from amplitude multilook images: we took into account, for each pixel, the ratio *s* between the mean of the image stack and its standard deviation. The PIF were located by choosing those pixels which have highest values of *s*. An example of the results for PIF extracted as described above is shown in Figure 8. We finally applied the inversion procedure to PIF (Figure 9).

CONCLUSIONS

Displacements obtained by inversion of InSAR data within the best PIF areas allowed us to recognise both long term, low velocity subsidence processes (about 20-30 mm for the 1992-2003 time span) and recurrent short term (seasonal) subsidence and rebound displacements (about 10-20 mm). The latter phenomena can be better recognised from 1996 to 1999, probably as effect of interferograms coherence. The results reasonably agree with leveling data, which provide maximum subsidence values of about 35 mm for the 1995-2005 time span. Peaks of seasonal vertical ground displacements inferred in Figure 9 are strongly correlated to peaks of seasonal water table variations (Figure 2). The results suggest that the aquifer under study probably is subjected to unrecoverable consolidation connected to the long term water table depletion and near-elastic deformation caused by seasonal water table variations. Anyway, considering the significant spatial and temporal decorrelation of InSAR ERS 1/2 data within the study area, the above hypothesis should be checked. So interesting topics for future investigations could be estension of InSAR analysis to ENVISAT, leveling measurements with higher temporal resolution and ground vertical displacement monitoring by means of extensometers.

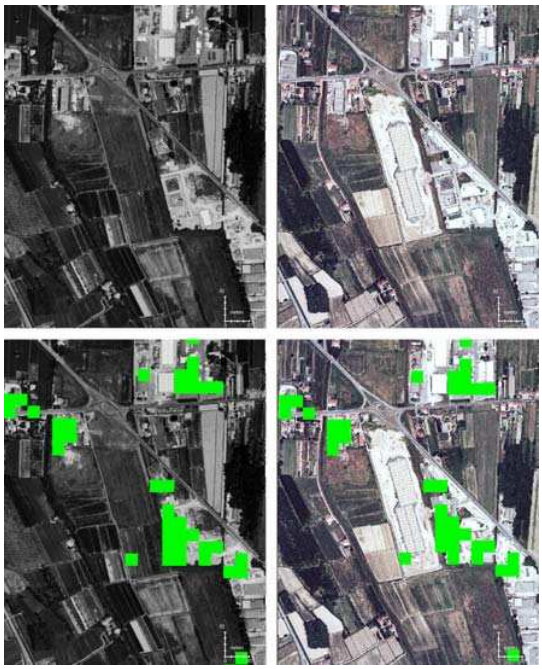

Figure 8. Location of PIF (green pixels) over orthophotos related to '94 (left) and '00 (right).

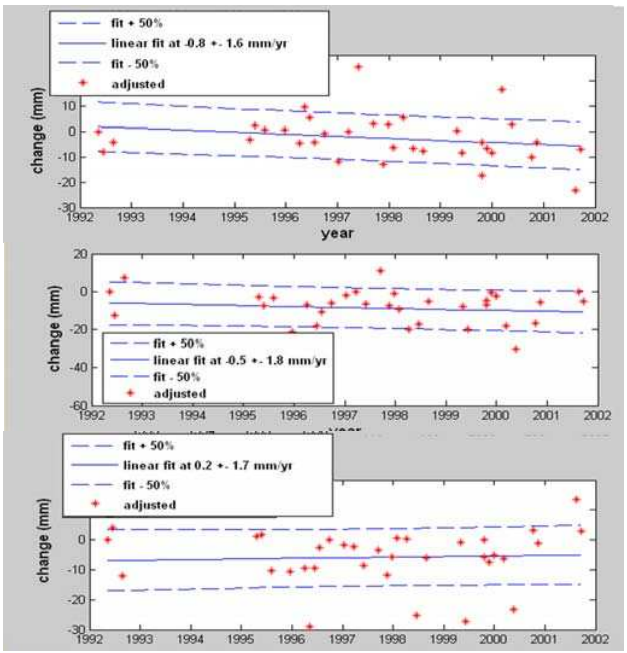

Figure 9. Examples of displacements calculated from InSAR for selected PIF.

BIBLIOGRAPHY

Feigl, K. L., J. Gasperi, F. Sigmundsson, and A. Rigo (2000), Crustal deformation near Hengill volcano, Iceland 1993-1998: coupling between volcanism and faulting inferred from elastic modeling of satellite radar interferograms, *J. Geophys. Res*, *105*, 26,555-525,670.

Massonnet, D., and K. L. Feigl (1998), Radar interferometry and its application to changes in the earth's surface, *Review of Geophysics*, *36*, 441–500.

Muller, G. (1986), *Appunti di livellazione*, I.G.M. Firenze.

Usai, S. (2003), A least squares database approach for SAR interferometric data, *IEEE Trans. Geoscience Rem. Sens.*, *41*, 753-760.